

# Actor Conditioned Attention Maps for Video Action Detection

Oytun Ulutan  
University of California, Santa Barbara  
Mudhakar Srivatsa  
IBM T. J. Watson Research Centre

Swati Rallapalli  
IBM T. J. Watson Research Centre  
B.S. Manjunath  
University of California, Santa Barbara

## Abstract

Interactions with surrounding objects and people contain important information towards understanding human actions. In order to model such interactions explicitly, we propose to generate attention maps that rank each spatio-temporal region's importance to a detected actor. We refer to these as Actor-Conditioned Attention Maps (ACAM), and these maps serve as weights to the features extracted from the whole scene. These resulting actor-conditioned features help focus the learned model on regions that are important/relevant to the conditioned actor. Another novelty of our approach is in the use of pre-trained object detectors, instead of region proposals, that generalize better to videos from different sources. Detailed experimental results on the AVA 2.1 datasets demonstrate the importance of interactions, with a performance improvement of 5 mAP with respect to state of the art published results.

## 1. Introduction

**Motivation:** Human action detection is a promising research field which has the potential to significantly improve applications such as surveillance, robotics, health-care and autonomous driving. While many existing datasets (e.g., UCF-101[34], HMDB-51[21], Kinetics[19]) are very useful for video search and classification, a more recent AVA[11] dataset focuses on atomic actions within short video segments. Such atomic actions have the potential to generalize to different contexts, become building blocks for more complex actions and improve the general understanding of human actions/interactions in videos. In this work we focus on the AVA dataset, as our primary goal is to create generalizable video action models while explicitly modeling actor interactions with the environment.

**Challenges:** In activity detection not only are the features related to the object (actor) alone important but also the interactions of actors with the surrounding context. This is especially true in the case of atomic activities, such as listen-

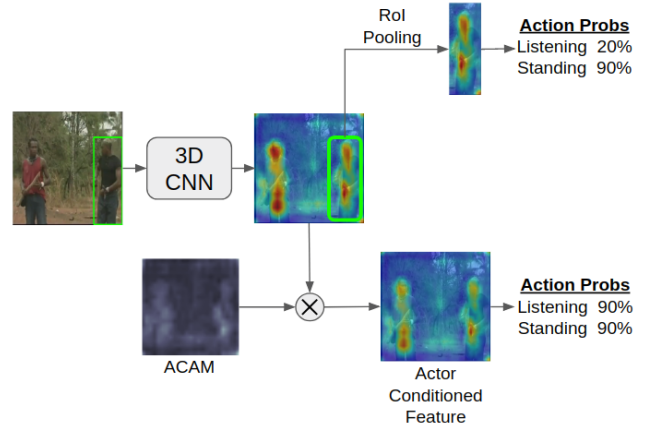


Figure 1. Comparing the Region of Interest(RoI) pooling with the proposed Actor Conditioned Attention Maps (ACAM) method for action detection. Even though the cropped feature map from the RoI Pooling sees a larger receptive field, it loses the additional information about the surroundings. Our method, ACAM, generates attention maps that are specific to each detected actor which multiplies the feature map to obtain the Actor Conditioned Features. Sum of activations across feature dimensions are visualized.

ing to a person, as cues from the scene may not aid the detection problem. This is in contrast to contextual activities like “swimming” where presence of water is a strong signal, or “skiing” where snow is a strong indicator. Recent works for action detection task have followed the ideas from the R-CNN architectures and extended it to videos[11, 26, 29, 33]. However, during such action detection, the bounding box locates the *actor* rather than the *action* itself. Even though the receptive field of such regions cropped from the feature maps are large, they do not explicitly model the varying amount of object/actor interactions occurring in different activities. In order to address this issue, we propose an improvement on region of interest pooling for action detection as demonstrated in Figure 1.

**Approach:** Contextual modeling has been used in recent works. Non-local Neural Networks [38] have modeled the

contextual information by generating a weighted sum of global features at every feature location which compresses the surrounding scene context. Research in Visual Question Answering [5, 24, 40] used attention maps to model relevant interactions in an image and focus the model to be able to answer questions. Actor-Centric Relations Network [35] modeled relations of actors by generating contextual features for each detected actor.

Inspired by such works, the proposed model generates attention maps *conditioned on each actor from contextual features and actor locations*. Attention maps are generated for each feature dimension and determine how relevant every feature location is to that conditioned actor. Such attention mechanism allows us focus on the actor without the Region of Interest Pooling (RoIPooling) operation and contain the spatio-temporal structure of the scene.

We summarize the main **contributions** below.

- **Generation of Actor Conditioned Attention Maps (ACAM):** We propose an attention model for person action detection that generates different attention maps for each actor in the scene.
- **Actor Conditioned Features:** Replacing the traditional region cropping for each actor, the generated attention maps are multiplied with the global feature map in order to generate an order-preserving feature representation for each actor.
- **Object detectors as high quality and generalizable RPNs:** Instead of retraining an RPN on the dataset, we use a pre-trained object detector to obtain quality actor locations and demonstrate that it is more generalizable to unseen data.

Codes will be made available at [Github](#). A real-time demo is also available at [Demo Repo](#).

## 2. Related Work

State of the art models on typical action recognition datasets [34],[21], [31] use architectures such as Two-Stream networks [32] combining RGB with Optical Flow, 2D Convolutions with LSTMs [43] and 3D Convolutions [13]. The release of the large-scale, high quality datasets like Sports 1M [18], Kinetics [19], allowed deeper 3D CNN models such as C3D [36], Inception 3D (I3D) [3] to be trained and these models achieved high performance. More recent works have focused on temporal action detection from untrimmed videos (e.g., ActivityNet [6], THUMOS [16]) using two-Stream 2D Convolutions [44], LSTMs [42] and 3D Convolutions [30].

The recent Atomic Visual Actions (AVA v2.1) [11] dataset exhaustively annotates the atomic actions and spatial locations of all the actors in complex scenes. Initial

methods on the AVA dataset extended the Faster-RCNN [27] architectures to 3D convolutions where initial layers generate actor proposals and each proposal is further analyzed by the following layers [11]. Recently published Actor Centric Relation Network (ACRN) [35] model generated features that combine proposal features with scene features to represent actor’s interactions with surrounding context. Our proposed model improves the ACRN model by adding an attention mechanism and generating feature maps from the whole scene conditioned on the actor. This architecture allows modeling of interactions between actors and objects.

Attention models have been used in the Natural Language Processing [28, 2, 37]. [37] implemented an attention function for relating different positions of a single sequence in sentences. Recently, combining NLP with Computer Vision, some works in the Visual Question Answering area focused on generating attention maps from the input question to focus the attention of visual model [5, 24, 40]. Attention maps have also been used in object detection methods. [14] used an object relation module to detect relation between objects which improves both instance recognition and duplicate removal. [22] used an LSTM structure to generate an attention map for modeling contextual information. In [38] a compact feature representation that compresses non-local information from contextual features is generated using a weighted sum of pixels, similar to an attention map.

Contextual information has also been studied on the recent image action detection datasets. Datasets such as V-COCO [12] and HICO-Det [4] have exhaustive annotations on persons, objects and their interactions. This allows models on such datasets to be able use such information and model interactions efficiently. Recently, [10] modeled interactions by using a multi-stream network where streams focused on persons, objects and interactions separately and achieved state of the art results.

## 3. Actor Conditioned Attention Maps

The objective in this work is to detect bounding boxes for each actor from a video segment and to classify the actions which can include any number of person poses, person-person interactions and person-object interactions. Instead of the traditional region proposal network (RPN) approach, actor bounding boxes are detected using a pre-trained and frozen object detector as this generates high-quality and generalizable bounding boxes.

Traditionally, given the bounding boxes, a region of interest representing the actor is cropped from the convolutional feature maps and further analyzed for actions. However, such methods do not explicitly model the interactions of actors with the surrounding context (objects, actors, scene). *We propose to model such interactions using attention maps conditioned on each detected actor*. These atten-

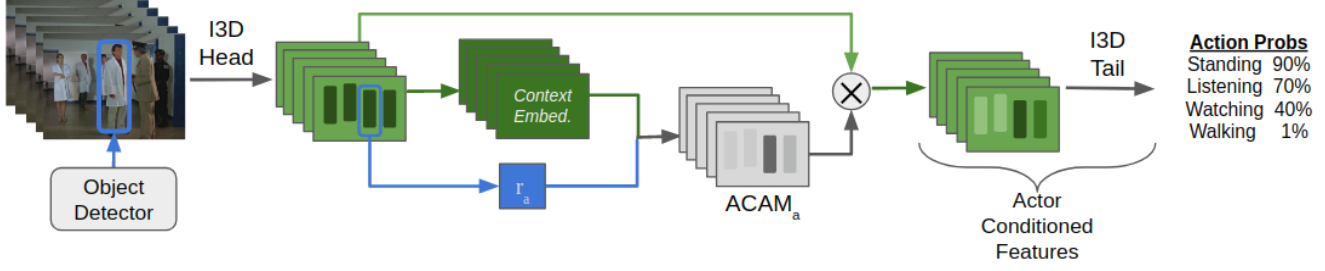


Figure 2. Actor Conditioned Attention Maps architecture. Each video segment initially goes through 3D convolutions. Actor locations are detected by a pre-trained from object detector. Feature vectors for each detected actor are generated from their locations on the feature map. Combining the actor feature vectors with contextual features extracted from the whole scene, a set of weights are generated for every spatio-temporal region in the scene. These weights, i.e. attention maps, are multiplied with the initial feature map and the resulting product represents the actor while modeling the interactions with the scene.

tion maps serve as weights to higher level features extracted from the whole input scene and quantify the importance of each spatio-temporal region to the conditioned actor. This allows attention maps to amplify features at regions that are relevant to the current actor while weakening the locations with less relevance. These conditioned features represent the actor while keeping the spatio-temporal ordering intact which allows the following convolutional layers to exploit the relative locations of objects and actors. Fig. 2 shows the proposed model architecture.

### 3.1. Object Detector as RPN

As mentioned earlier, unlike traditional action detection approaches, we use a pre-trained, frozen, object detector for detecting regions of interest within video frames. This approach has the following advantages:

**Generalizability:** While training object detectors, the models see large variations in objects from large datasets such as MS-COCO [23]. This allows object detectors trained on object detection datasets to generalize well to videos from other sources such as surveillance videos and robotic cameras. Compared to these datasets, large action datasets usually come from similar sources such as AVA (Movies), JHMDB (Youtube). Even though they vary in action dynamics, they do not have enough variations in views of actors.

**High Quality Actor Region Proposals:** Using ACAM feature representation for each actor proposal requires more memory compared to using RoI pooling. In order to train the model efficiently, fewer number of higher quality region proposals are essential and these can be obtained using pre-trained object detectors.

### 3.2. Actor Conditioned Attention Features

Compared to object detection tasks, action boundaries are not as well defined and can include interactions with other objects and actors. Additionally, different actions require different sizes of visual areas to be considered from

the input video. For example, “walking” action requires the model to consider only the pixels on the actor and its close surroundings whereas “listening a person” action requires the model to look for the larger context around the actor in addition to the actor itself. With such variety in action classes, using traditional object detection methods such as RoIPooling can potentially lose the contextual information around the actors. Even though features cropped using RoIPooling do include information from a larger receptive field, it compresses that information into a smaller feature map which loses the spatio-temporal ordering of the surroundings and does not explicitly model interactions (with other actors or objects). In order to address these challenges, we propose a model where attention maps are generated for each detected actor and these attention maps model the importance of each spatio-temporal region in the feature map to the conditioned actor.

Similar to Faster RCNN [27] architectures, initially the input video  $V$  goes through convolutions and a spatio-temporal feature tensor  $I$  ( $T \times H \times W \times C_I$ ) is generated:

$$I = 3D\_CNN(V) \quad (1)$$

Using RoIPooling, for every actor  $a$  detected in the scene a fixed feature vector  $r_a$  ( $1 \times 1 \times 1 \times C_I$ ) is extracted from  $I$ :

$$r_a = RoIPooling(I, a) \quad (2)$$

Instead of the usual practice of using  $r_a$  for classification [11], we want to generate a set of weights that quantify the actor  $a$ ’s relation to every spatio-temporal region and every feature channel within the global feature map  $I$ . These sets of weights,  $ACAM_a$ , are the attention maps of actor  $a$  on features  $I$ .

To generate the attention maps, initially, a context embedding is generated from each location in the global feature map  $I$ :

$$E_{t,i,j} = e_{\theta}(I_{t,i,j}) \quad (3)$$

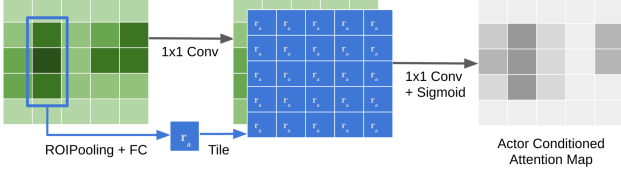


Figure 3. Generation of attention maps. From each actor’s location a fixed length feature vector is extracted. This feature vector is tiled and concatenated to features extracted from the whole scene at every spatio-temporal location. This combined feature vector allows modeling of interactions. A sigmoid function is used to force the weights into  $[0, 1]$  interval.

These embeddings can be efficiently implemented using  $1 \times 1 \times 1$  convolutions. Combining the context embedding vector  $E_{t,i,j}$  with the actor feature vector  $r_a$ , attention map conditioned on actor  $a$  can be obtained by:

$$ACAM_{t,i,j} = \sigma(g_\phi(r_a, E_{t,i,j})) \quad (4)$$

Where  $\sigma$  is the sigmoid function and  $g_\phi$  is an embedding that combines actor feature  $r_a$  at every spatio-temporal location of context embedding vector  $E_{t,i,j}$ . Note that actor feature vector  $r_a$ , is independent of the time and space indices  $(t, i, j)$  and is repeated across these dimensions.

Fig. 3 shows the generation of the attention map. The attention maps are generated for every feature channel  $C_I$  and determines the actor’s relation/relevance of features at each location. Having an attention map for every channel allows the model to capture different types of actor-action interactions.

Final feature map representing the actor can be generated by multiplying the attention map with the input feature at every location, i.e., elementwise product:

$$F_{t,i,j} = I_{t,i,j} \cdot ACAM_{t,i,j} \quad (5)$$

Compared to the usual practice of cropping the feature map on actor’s location, this feature  $F_{t,i,j}$  is the same shape as the input feature map  $I_{t,i,j}$  and includes information of the whole scene. By multiplying the input feature with an attention map conditioned on the actor, the feature  $F_{t,i,j}$  is now a representation of the actor and able to model the interactions with the surrounding spatio-temporal regions. This allows us to feed the feature map  $F$  into the remaining convolutional layers in I3D and classify the action of the conditioned actor.

## 4. Experiments and Evaluation

### 4.1. Dataset and Implementation Detail

**Dataset:** The proposed model is tested on the AVA v2.1 dataset. AVA dataset contains of 2 second video segments of multiple actors in each segment. Each actor can have

multiple action labels in each segment. For evaluation we follow the AVA v2.1 benchmark and calculate the mean Average Precision (mAP) across the 60 benchmark classes. The action classes are split into 3 larger categories Person Poses (13 classes), Person Object Interactions (32 classes), Person Person Interactions (15 classes). In this release, dataset consists 211k Training and 57k Validation samples.

**3D CNNs:** We use I3D [3] model as a 3D CNN backbone for all of our models. In our model, the input video segment goes through initial I3D layers until the “Mixed\_4f” layer and the context feature vector  $I$  is obtained. From the “Mixed\_4f” feature map, actor features  $r_a$  and context embedding  $E$  is extracted. Combining these features, the final feature map  $F$  is generated. Since the  $F$  is the original feature map  $I$  multiplied with a set of weights  $ACAM$ , remaining I3D layers can be efficiently used and initialized with pre-trained weights. We use the remaining layers up to final “Mixed\_5c” and call this operation “I3D Tail”. Additionally, a global average pooling across spatio-temporal dimensions is applied to the final feature map. This allows us to efficiently model the scene. From the 2 second videos, we subsample 32 frames by taking every other frame.

**Actor Detection:** Initially we run the object detector on all of the videos and save the detected actors. We use the Faster R-CNN model [27] with NAS [46] feature extractor that was pre-trained on MS-COCO [23] dataset. These object detectors are further analyzed in [15] and available within Tensorflow Object Detection API. We change the available default configuration such that it allows batch processing and it only filters out object bounding boxes with less than 1% confidence (Default 30%) as AP metric requires to rank the low confidence detections as well.

**Augmentations:** In addition to usual cropping and flipping of the input video sequences, we augment the bounding box coordinates received from the object detector. This allows the model to be less dependent on the object detector and allows object detector to be switched with a faster detector during test time.

**Training:** We initialize our models with I3D weights trained on Kinetics-400 dataset [3]. We train our models with Adam optimizer [20] and a learning rate of 0.01 for 20 epochs. We use a batch size of 2 per GPU and use 4 1080Ti for training. Batch-norm updates are disabled and initialized values are used. Tensorflow [1] Framework is used to implement all the models.

### 4.2. Comparisons with the State of the Art

We compare our model with the state of the art Action Detection models on the AVA v2.1 dataset. Table 1 shows that compared to the current highest performing paper ACRN [35], our ACAM model improves performance of validation set by  $5mAP$ .

Additionally, we compare our model with the valida-



Model Architecture	AVA v2.1 Validation mAP
Single Frame[11]	14.20
I3D [11]	15.10
ACRN [35]	17.40
<b>ACAM - ours</b>	<b>22.52</b>

Table 1. Validation mAP results compared to published state of the art results. Proposed model ACAM achieves the highest performance on the AVA v2.1 Validation set.

Model Architecture	AVA v2.1 Validation mAP
YH Technologies[41]	19.40
Megvii/Tsinghua[17]	20.01
Deep Mind[9]	21.90
<b>ACAM - ours</b>	<b>22.52</b>

Table 2. Validation mAP results compared to the models from the ActivityNet CVPR-2018 AVA challenge. We only included the single model - RGB methods instead of the ensembles/fusions as we are comparing benefits of the proposed layer.

tion results of the models from the ActivityNet 2018 AVA challenge[8]. Table 2 shows that our model achieves the best performance in validation among these models as well. In this table, we exclude results from ensemble/fusion models and compare with their highest performing single model. This is because, our goal is to demonstrate the benefit of the ACAM layer, which can be used in place of the RoIPooling layer in each of the individual models of the ensemble.

In order to compare with the challenge models, we implement a model similar to the Deep Mind [9] model. This model is explained further in next section and is called “3D Head + RoIPool + I3D Tail”. As the model weights and code from the challenge is not available, our implementation achieves 19.83 mAP. This performance compared to ACAM’s 22.52, demonstrates that the proposed ACAM method is complementary to such architectures that use RoIPooling for action detection and would increase the performance of [9] further.

### 4.3. Comparisons of Individual Modules

The proposed model architecture consists of multiple modules. In this section, we demonstrate the purpose of each module and experiment with alternative models to ACAM for representing contextual interactions. Results for these different implementations are shown in Table 3.

**I3D Head + RoIPool (Base Model):** Our first implementation follows the model from [11]. The input video segment goes through I3D convolutions upto the layer “Mixed\_4f”, we call this implementation I3D Head. The context feature  $I$  is cropped on the actor’s location using traditional region of interest pooling and the actor feature vector  $\mathbf{r}_a$  is obtained. Fully connected layers are used to get the final action results. In our implementation, this model achieves

Model Architecture	AVA v2.1 Validation mAP
I3D Head + RoIPool (Base)	18.01
I3D Head + RoIPool + Tail	19.83
I3D Head + ACRN + Tail	20.59
I3D Head + NL-RoI + Tail	20.82
<b>I3D Head + ACAM + Tail</b>	<b>22.52</b>

Table 3. mAP results of our different implementations.

Model Architecture	Pose	Objects	Interaction
I3D Head + RoIPool	36.88	9.87	19.02
I3D Head + RoIPool + Tail	38.45	12.11	20.16
I3D Head + ACRN + Tail	38.38	12.52	22.37
I3D Head + NL-RoI + Tail	40.50	12.06	22.45
<b>I3D Head + ACAM + Tail</b>	<b>42.54</b>	<b>13.29</b>	<b>23.46</b>

Table 4. mAP results on different action categories defined by the dataset. Pose: Person Pose actions (ex: walking, standing), Objects: Object Manipulation actions (ex: drink, pull), Interaction: Person Interaction actions (ex: talk to a person, watch a person).

18.01 mAP and is our base model for comparisons.

**I3D Head + RoIPool + I3D Tail:** Similar to the previous model, we crop the actor’s location from the context feature  $I$  using RoI Pooling. However, instead of the fully connected layers, we use the rest of the I3D layers from “Mixed\_4f” to “Mixed\_5c” as explained in the previous section. This method achieves 19.83 mAP and demonstrates that using I3D Tail improves the performance by 2 mAP.

**I3D Head + NL-RoI + I3D Tail:** Recently, Non-Local Neural Networks [38] model used a compact representation of features which is able to model interactions between different spatio-temporal regions in a video segment. We modify this model such that non-local features are generated between the detected actor features  $\mathbf{r}_a$  and scene context features  $I$ . This model generates a compact fixed sized feature map which is the weighted sum of regions in  $I$ . This model achieves 20.82 mAP and improves the performance by 1 mAP compared to RoI pooling.

**I3D Head + ACRN + I3D Tail:** From the ACRN work [35], we implement the context relation module without the added  $3 \times 3$  from the paper. In addition to their implementation, we process the combined contextual feature map with I3D Tail. This model improves the performance by 1 mAP.

**I3D Head + ACAM + I3D Tail:** This model uses the proposed Actor Conditioned Attention Maps module for representing the actors. Compared to the alternative contextual relation models, the proposed model achieves the highest performance. Combining the ACAM contextual model with I3D Tail achieves the highest performance.

The breakdown of performance per action category is demonstrated in Table 4. The categories are defined by the AVA dataset [11]. AP values are averaged across category classes to obtain these results. This demonstrates that

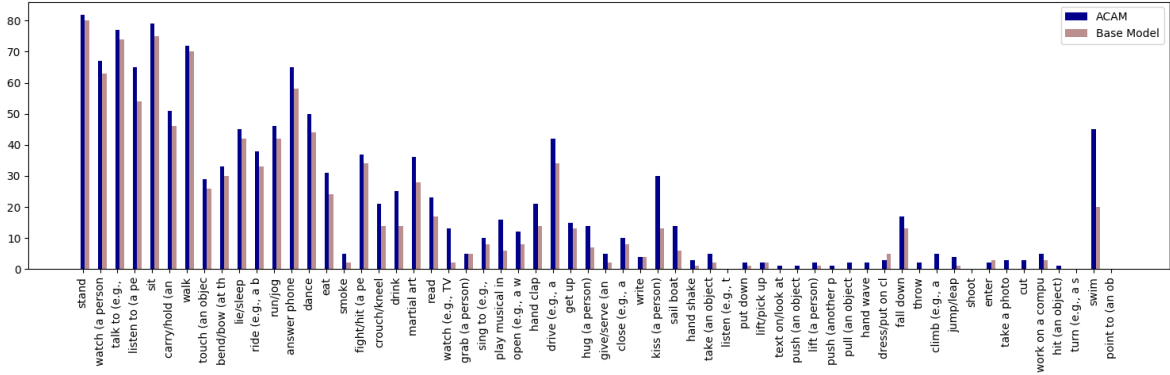


Figure 4. Per class AP results for the proposed ACAM model and the base model I3D Head + RoIPool. The classes are sorted by the number of training samples available in the dataset.

the models that explicitly use contextual information improve the performance in Person-Person Interaction actions whereas the proposed model ACAM is able to additionally improve object interactions as well.

Additionally, Figure 4 shows the per class breakdown of the performances between the proposed ACAM model and the base model model. We observe a improvement in classes such as drive, sail boat where context is very helpful and passive actions such as listen to a person, watch a tv where the context is active instead of the actor.

#### 4.4. Ablation Analysis

**Actor Detection Performance:** To test the performance of the object detector, we calculate the detection AP of every actor for every class on AVA v2.1 validation set. Averaging the detection result across classes instead of across number of samples allows us to accurately evaluate the detection rate for this task as there is a large variation in number of samples of each class. Table 5 shows the detection frame AP scores for the AVA v2.1 validation set.

Object Detector	AVA Actor Detection AP
F RCNN-NAS	97.10
F RCNN-Resnet101	95.97
SSD - IncpV2	66.16

Table 5. AP results for actor detection rate for different object detectors.

**Generalizable Actor Detection:** The main reason of using a pre-trained frozen object detector instead of training an RPN on the action dataset is generalizability. During training, object detectors see large variations in objects from large datasets such as MS-COCO [23] compared to action datasets. This makes object detectors more generalizable compared to retrained RPNs. To test this hypothesis, we compare the actor detection rates of same model architec-

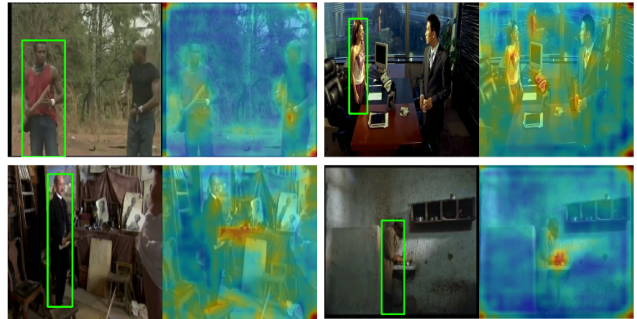


Figure 5. Generated Actor Conditioned Attention Maps. Higher attention values are usually observed around objects (paper, chairs, teapot, phones), on faces and hands of the actors.

ture trained on COCO and AVA datasets. Table 6 shows their comparisons on different datasets. Even though they have similar detection rates on the AVA datasets, the model trained on AVA does not generalize to other datasets such as VIRAT[25] and KITTI [7] as the actor detection significantly deteriorates on these datasets.

Actor Detection Rate	F RCNN COCO	F RCNN AVA
AVA	95.97	93.02
VIRAT	30.44	9.94
KITTI	54.57	27.04

Table 6. AP results for actor detection rate of the same object detector trained on AVA and COCO and tested on different datasets.

**Visualization of Attention Maps:** In ACAM, an attention map for each feature channel is generated. This allows us to model different types of interactions efficiently. Since the feature maps are sparse, visualization of attention maps is challenging. Therefore, in order to visualize them, we average the attention map values across the feature dimension where they have non-zero values in their respective feature

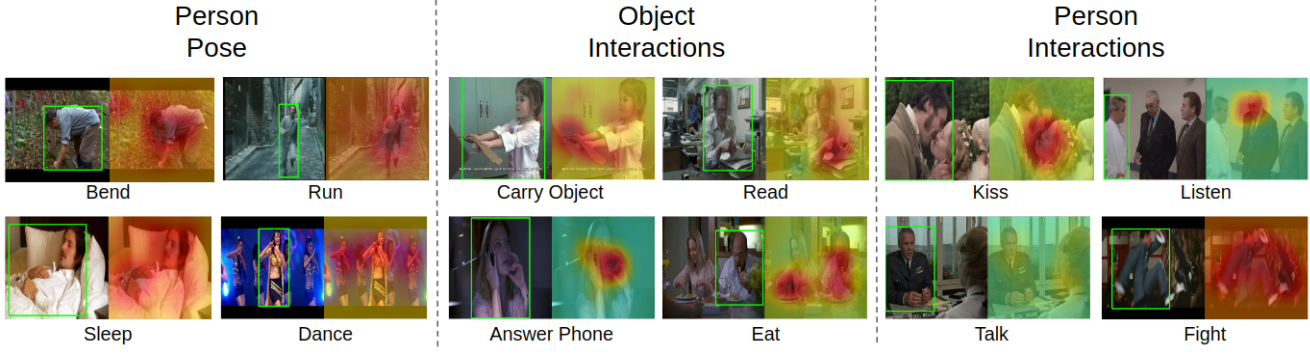


Figure 6. Class activation maps for detected actors. Each row represents the activation maps for the actor annotated by the green bounding box. Red regions on the activation maps represent the higher values. Segments are taken from validation set.

map. This generates a representation where each actor’s relation with the scene is visible. Figure 5 shows this visualization on different examples. Note that a higher attention value is obtained on objects and actor faces/hands.

**Class Activation Maps:** Since our model has a global pooling layer at the last layer before the fully connected classification layers, we are able to easily generate class activation maps for each class similar to [45]. We generate activation maps for several different cases available in the dataset. Figure 6 shows activation maps for different categories of actions. Activation maps are shown for actors annotated in green bounding boxes. Maximum activation across timesteps is shown in the figures for visualization as these feature maps are also a time sequence.

We observe that pose actions such as run/bend get activated around the actor while object interaction actions such as carry object/eat are activated around the relevant objects and the actors. Person interactions also show some interesting results. The passive actions such as “watch a person”, “listen to a person” gets activated where there is another person in the scene that is “talking” or relevant.

Figure 7 shows a scene with three people and their conditioned activation maps for specific actions. Each row represents the activation maps that are conditioned on the person in the green bounding box. We observe that complementary actions such as “talking” and “listening” gets activated on the person with the opposite action. This is due to our model architecture. As we initially extract the actor feature vector  $r_a$  from the actor’s location, this feature vector contains the information that the current actor  $a$  is “listening”. Therefore the attention map generated from actor’s vector  $r_a$  and context embedding  $E$  looks for a person that is “talking” and focuses the attention on those locations.

**Single attention map vs per feature channel attention map:** Works modeling contextual interactions such as [38] use a single function to model interactions between two points. However, this prevents the model from detecting dif-

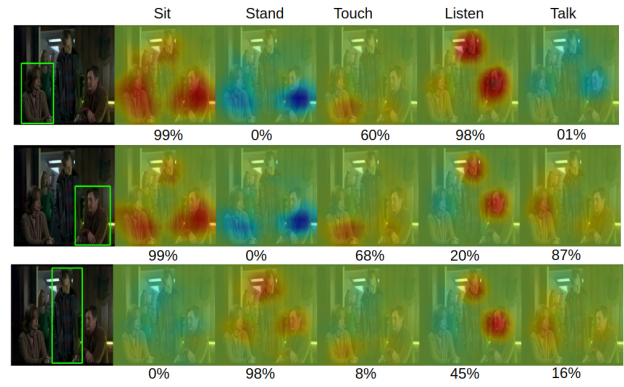


Figure 7. Class activation maps for detected actors. Each row represents the activation maps for the actor annotated by the green bounding box. Person on the right is talking in the video. Red regions on the activation maps represent the higher values. Segments are taken from validation set.

ferent types of interactions. In order to address this issue, instead of generating a single attention map in our work, we generate the attention maps per feature channel. When trained with a single attention map that multiplies the input feature map  $I$ , the model was unable to distinguish between different actors in the scene and generated same confidence values for every actor.

#### 4.5. End to End Framework for Action Detection

In order to test the generalizability and the performance of the proposed model on different datasets qualitatively, we implement an end-to-end framework for detecting and tracking actors and analyzing their actions.

We combine the object detector with the Deep Sort[39] model. Deep Sort is a simple tracking/re-identifying model that uses a deep association metric for matching detected person bounding boxes. This allows us to track the detections over time and generates person tubelets.



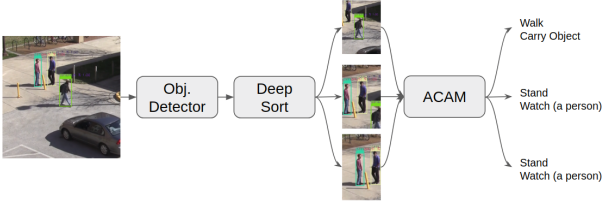


Figure 8. ACAM video action detection framework running on a surveillance video from VIRAT[25] dataset. The actors are detected by object detectors and tracked over frames by the Deep Sort model. The generated tubes for each person is used by the ACAM action detector to analyze their actions.

Since the proposed model explicitly models the surrounding context, a larger area than the person’s tubelet is essential in modeling interactions. Due to the large view of surveillance videos, it is not feasible to process the whole scene. For this reason, square regions centered on the person’s location and twice the size of the person’s area are cropped and fed into the action detection framework.

Figure 8 shows the overall pipeline of the system. First, actor tubes with a larger context are extracted from the video using the detector and the tracker. Then, each detected tube is analyzed by the ACAM module for actions. Input frame and cropped tubes for each actor are visualized from the VIRAT[25] surveillance dataset. Notice that in cases such as “watching a person” model benefits from having a person in the surrounding context. We provide more qualitative results on Figure 9 with results on autonomous driving dataset KITTI[7] tracking, surveillance dataset VIRAT and other videos from Youtube - UCF101[34].

A real-time version of this pipeline is available at [Demo Repo](#). It achieves 16 frames per second through a webcam using a single Nvidia GTX 1080Ti gpu.

## 5. Discussions

### 5.1. Comparisons of Attention Mechanisms

Our work is inspired by works Actor-Centric Relation Network (ACRN) [35], Non-Local Neural Networks (NL) [38] and Attentive Contexts for Object Detection (ACOD) [22]. In this section, we analyze the differences of these works to our proposed model and address their shortcomings for this specific task of action detection.

The most recent work that also models action detection is the ACRN [35] where the contextual information is extracted similar to our work. ACRN combines the actor features with contextual features and trains an additional convolutional layer for classification. In contrast, we combine actor and contextual features to generate a set of weights for the original features. These weights characterize the actor-action relationships while preserving the original fea-



Figure 9. ACAM video action detection framework qualitative results on videos from different sources. Top left: VIRAT surveillance dataset[25], Top right: UCF101[34]- Youtube, Bottom: KITTI [7] tracking autonomous driving dataset.

tures which allows the use of remaining convolutional layers from the CNN backbone.

The ACOD work [22] generates a single attention map using LSTMs for exploiting contextual information in object detection. For action detection, however, a single attention map is insufficient as feature maps represent more complicated relations. For example “listening” action might look for other “talking” people whereas, “carrying object” looks for objects. Attention mechanisms in such cases need to model these differences separately. This is the reason we are generating separate attention maps for each feature channel. Additionally, since the actor is detected, it is beneficial to generate the attention maps by using the information from the actor’s location.

The NL [38] work generates weighted means of the whole scene at every pixel location in the feature map for action recognition. This allows the model to compress the relevance between every pixel pair. In contrast, the proposed actor-conditioned ACAM generates a representation for actor/scene interactions in a higher level in forms of attention maps. Since the actor bounding box is known, representing that location with a vector makes more sense than looking for every pixel location on the sparse actor feature map. Additionally, since it is a weighted sum, a softmax function is used in the generation of weights. This limits the number of available interactions as different relations will be competing with each other, in contrast to a sigmoid.

### 5.2. Conclusion

We presented a novel action detection model that explicitly captures the contextual information of an actor’s surroundings. Our method, ACAM, uses attention maps as a



set of weights to focus on the spatio-temporal regions that are relevant to the actor. This works as a replacement for RoIPooling method and is more suited for preserving interactions with objects and other actors. We test the effectiveness of our model via detailed evaluations and find that it improves the accuracy by 5 mAP over the state-of-the-art published results.

## References

- [1] M. Abadi, A. Agarwal, et al. TensorFlow: Large-scale machine learning on heterogeneous systems, 2015. Software available from tensorflow.org. **4**
- [2] D. Bahdanau, K. Cho, and Y. Bengio. Neural machine translation by jointly learning to align and translate. *arXiv preprint arXiv:1409.0473*, 2014. **2**
- [3] J. Carreira and A. Zisserman. Quo vadis, action recognition? a new model and the kinetics dataset. In *Computer Vision and Pattern Recognition (CVPR), 2017 IEEE Conference on*, pages 4724–4733. IEEE, 2017. **2, 4**
- [4] Y. Chao, Y. Liu, X. Liu, H. Zeng, and J. Deng. Learning to detect human-object interactions. *arXiv preprint*. **2**
- [5] A. Das, H. Agrawal, L. Zitnick, D. Parikh, and D. Batra. Human attention in visual question answering: Do humans and deep networks look at the same regions? *Computer Vision and Image Understanding*, 163:90–100, 2017. **2**
- [6] B. G. Fabian Caba Heilbron, Victor Escorcia and J. C. Niebles. Activitynet: A large-scale video benchmark for human activity understanding. In *Proceedings of the IEEE Conference on Computer Vision and Pattern Recognition*, pages 961–970, 2015. **2**
- [7] A. Geiger, P. Lenz, and R. Urtasun. Are we ready for autonomous driving? the kitti vision benchmark suite. In *Conference on Computer Vision and Pattern Recognition (CVPR)*, 2012. **6, 8**
- [8] B. Ghanem, J. C. Niebles, C. Snoek, F. C. Heilbron, H. Alwassel, V. Escorcia, R. Khrista, S. Buch, and C. D. Dao. The activitynet large-scale activity recognition challenge 2018 summary. *arXiv preprint arXiv:1808.03766*, 2018. **5**
- [9] R. Girdhar, J. Carreira, C. Doersch, and A. Zisserman. A better baseline for ava. *arXiv preprint arXiv:1807.10066*, 2018. **5**
- [10] G. Gkioxari, R. Girshick, P. Dollár, and K. He. Detecting and recognizing human-object interactions. *arXiv preprint arXiv:1704.07333*, 2017. **2**
- [11] C. Gu, C. Sun, D. A. Ross, C. Vondrick, C. Pantofaru, Y. Li, S. Vijayanarasimhan, G. Toderici, S. Ricco, R. Sukthankar, et al. Ava: A video dataset of spatio-temporally localized atomic visual actions. In *IEEE Conference on Computer Vision and Pattern Recognition, CVPR*, 2018. **1, 2, 3, 5**
- [12] S. Gupta and J. Malik. Visual semantic role labeling. *arXiv preprint arXiv:1505.04474*, 2015. **2**
- [13] R. Hou, C. Chen, and M. Shah. Tube convolutional neural network (t-cnn) for action detection in videos. In *IEEE international conference on computer vision*, 2017. **2**
- [14] H. Hu, J. Gu, Z. Zhang, J. Dai, and Y. Wei. Relation networks for object detection. In *Computer Vision and Pattern Recognition (CVPR)*, volume 2, 2018. **2**
- [15] J. Huang, V. Rathod, C. Sun, M. Zhu, A. Korattikara, A. Fathi, I. Fischer, Z. Wojna, Y. Song, S. Guadarrama, et al. Speed/accuracy trade-offs for modern convolutional object detectors. In *IEEE CVPR*, volume 4, 2017. **4**
- [16] H. Idrees, A. R. Zamir, Y.-G. Jiang, A. Gorban, I. Laptev, R. Sukthankar, and M. Shah. The thumos challenge on action recognition for videos in the wild. *Computer Vision and Image Understanding*, 155:1–23, 2017. **2**
- [17] J. Jiang, Y. Cao, L. Song, S. Z. Y. Li, Z. Xu, Q. Wu, C. Gan, C. Zhang, and G. Yu. Human centric spatio-temporal action localization. **5**
- [18] A. Karpathy, G. Toderici, S. Shetty, T. Leung, R. Sukthankar, and L. Fei-Fei. Large-scale video classification with convolutional neural networks. In *CVPR*, 2014. **2**
- [19] W. Kay, J. Carreira, K. Simonyan, B. Zhang, C. Hillier, S. Vijayanarasimhan, F. Viola, T. Green, T. Back, P. Natsev, et al. The kinetics human action video dataset. *arXiv preprint arXiv:1705.06950*, 2017. **1, 2**
- [20] D. P. Kingma and J. Ba. Adam: A method for stochastic optimization. *arXiv preprint arXiv:1412.6980*, 2014. **4**
- [21] H. Kuehne, H. Jhuang, E. Garrote, T. Poggio, and T. Serre. HMDB: a large video database for human motion recognition. In *Proceedings of the International Conference on Computer Vision (ICCV)*, 2011. **1, 2**
- [22] J. Li, Y. Wei, X. Liang, J. Dong, T. Xu, J. Feng, and S. Yan. Attentive contexts for object detection. *IEEE Transactions on Multimedia*, 19(5):944–954, 2017. **2, 8**
- [23] T.-Y. Lin, M. Maire, S. Belongie, J. Hays, P. Perona, D. Ramanan, P. Dollár, and C. L. Zitnick. Microsoft coco: Common objects in context. In *European conference on computer vision*, pages 740–755. Springer, 2014. **3, 4, 6**
- [24] J. Lu, J. Yang, D. Batra, and D. Parikh. Hierarchical question-image co-attention for visual question answering. In *Advances In Neural Information Processing Systems*, pages 289–297, 2016. **2**
- [25] S. Oh, A. Hoogs, A. Perera, N. Cuntoor, C.-C. Chen, J. T. Lee, S. Mukherjee, J. Aggarwal, H. Lee, L. Davis, et al. A large-scale benchmark dataset for event recognition in surveillance video. In *Computer vision and pattern recognition (CVPR), 2011 IEEE conference on*, pages 3153–3160. IEEE, 2011. **6, 8**
- [26] X. Peng and C. Schmid. Multi-region two-stream r-cnn for action detection. In *European Conference on Computer Vision*, pages 744–759. Springer, 2016. **1**
- [27] S. Ren, K. He, R. Girshick, and J. Sun. Faster r-cnn: Towards real-time object detection with region proposal networks. In *Advances in neural information processing systems*, pages 91–99, 2015. **2, 3, 4**
- [28] A. M. Rush, S. Chopra, and J. Weston. A neural attention model for abstractive sentence summarization. *arXiv preprint arXiv:1509.00685*, 2015. **2**
- [29] S. Saha, G. Singh, M. Sapienza, P. H. Torr, and F. Cuzzolin. Deep learning for detecting multiple space-time action tubes in videos. *arXiv preprint arXiv:1608.01529*, 2016. **1**
- [30] Z. Shou, D. Wang, and S.-F. Chang. Temporal action localization in untrimmed videos via multi-stage cnns. In *Proceedings of the IEEE Conference on Computer Vision and Pattern Recognition*, pages 1049–1058, 2016. **2**

- [31] G. A. Sigurdsson, G. Varol, X. Wang, A. Farhadi, I. Laptev, and A. Gupta. Hollywood in homes: Crowdsourcing data collection for activity understanding. In *European Conference on Computer Vision*, pages 510–526. Springer, 2016. [2](#)
- [32] K. Simonyan and A. Zisserman. Two-stream convolutional networks for action recognition in videos. In *Advances in neural information processing systems*, pages 568–576, 2014. [2](#)
- [33] G. Singh, S. Saha, M. Sapienza, P. H. Torr, and F. Cuzzolin. Online real-time multiple spatiotemporal action localisation and prediction. In *ICCV*, pages 3657–3666, 2017. [1](#)
- [34] K. Soomro, A. R. Zamir, and M. Shah. Ucf101: A dataset of 101 human actions classes from videos in the wild. *arXiv preprint arXiv:1212.0402*, 2012. [1](#), [2](#), [8](#)
- [35] C. Sun, A. Shrivastava, C. Vondrick, K. Murphy, R. Sukthankar, and C. Schmid. Actor-centric relation network. *arXiv preprint arXiv:1807.10982*, 2018. [2](#), [4](#), [5](#), [8](#)
- [36] D. Tran, L. Bourdev, R. Fergus, L. Torresani, and M. Paluri. Learning spatiotemporal features with 3d convolutional networks. In *Proceedings of the IEEE international conference on computer vision*, pages 4489–4497, 2015. [2](#)
- [37] A. Vaswani, N. Shazeer, N. Parmar, J. Uszkoreit, L. Jones, A. N. Gomez, Ł. Kaiser, and I. Polosukhin. Attention is all you need. In *Advances in Neural Information Processing Systems*, pages 5998–6008, 2017. [2](#)
- [38] X. Wang, R. Girshick, A. Gupta, and K. He. Non-local neural networks. In *The IEEE Conference on Computer Vision and Pattern Recognition (CVPR)*, 2018. [1](#), [2](#), [5](#), [7](#), [8](#)
- [39] N. Wojke, A. Bewley, and D. Paulus. Simple online and realtime tracking with a deep association metric. In *2017 IEEE International Conference on Image Processing (ICIP)*, pages 3645–3649. IEEE, 2017. [7](#)
- [40] Z. Yang, X. He, J. Gao, L. Deng, and A. Smola. Stacked attention networks for image question answering. In *Proceedings of the IEEE Conference on Computer Vision and Pattern Recognition*, pages 21–29, 2016. [2](#)
- [41] T. Yao and X. Li. Yh technologies at activitynet challenge 2018. *arXiv preprint arXiv:1807.00686*, 2018. [5](#)
- [42] S. Yeung, O. Russakovsky, N. Jin, M. Andriluka, G. Mori, and L. Fei-Fei. Every moment counts: Dense detailed labeling of actions in complex videos. *International Journal of Computer Vision*, 126(2-4):375–389, 2018. [2](#)
- [43] J. Yue-Hei Ng, M. Hausknecht, S. Vijayanarasimhan, O. Vinyals, R. Monga, and G. Toderici. Beyond short snippets: Deep networks for video classification. In *Proceedings of the IEEE conference on computer vision and pattern recognition*, pages 4694–4702, 2015. [2](#)
- [44] Y. Zhao, Y. Xiong, L. Wang, Z. Wu, X. Tang, and D. Lin. Temporal action detection with structured segment networks. *ICCV, Oct*, 2, 2017. [2](#)
- [45] B. Zhou, A. Khosla, A. Lapedriza, A. Oliva, and A. Torralba. Learning deep features for discriminative localization. In *Proceedings of the IEEE Conference on Computer Vision and Pattern Recognition*, pages 2921–2929, 2016. [7](#)
- [46] B. Zoph, V. Vasudevan, J. Shlens, and Q. V. Le. Learning transferable architectures for scalable image recognition. [4](#)